united nations
educational, scientific
and cultural
organization

international atomic
energy agency

the
abdus salam
international centre for theoretical physics

H4. SMR/1247
Lecture Note: 04

WORKSHOP ON PHYSICS OF MESOSPHERE-STRATOSPHERE-TROPOSPHERE INTERACTIONS WITH SPECIAL EMPHASIS ON MST RADAR TECHNIQUES

(13 - 24 November 2000)

RADAR INVESTIGATIONS OF THE MESOSPHERE, STRATOSPHERE AND THE TROPOSPHERE IN SVALBARD

Prof. Jurgen ROTTGER

Max-Planck-Institut fur Aeronomie
Katlenburg-Lindau
GERMANY

Adv. Polar Upper Atmos. Res., 14, ~~000-000~~, 2000
202-220

Radar Investigations of the Mesosphere, Stratosphere and the Troposphere in Svalbard

Jürgen Röttger

Max-Planck-Institut für Aeronomie
Max-Planck-Str. 2
D-37191 Katlenburg-Lindau
Germany

Abstract: This paper deals with observations of the mesosphere with the EISCAT Svalbard Radar (ESR) and of the middle and lower atmosphere (mesopause, lower stratosphere and troposphere) with the SOUSY Svalbard Radar (SSR), which are operated in the close vicinity of Longyearbyen on Spitzbergen/Svalbard. The scientific aims for studies of this altitude region are summarized. We briefly describe these radar systems and their operation principles. Examples of troposphere and lower stratosphere structure and dynamics, which are obtained with the SSR, are presented. First observations of Polar Mesosphere Summer Echoes with the SSR and the ESR are introduced. Meteor echoes detected with the SSR are briefly described and the first D-region observations with the ESR demonstrate its capability to perform observations down to altitudes below 60 km. Finally some ideas are put forward how to continue and establish collaborations for the use of the SSR in the coming years.

I01

1. Introduction

In the polar middle atmosphere phenomena from above, resulting from the effect of the solar wind on the Earth's ionosphere and atmosphere, and phenomena from below, such as tides and gravity waves propagating upwards from the troposphere, merge. The relative importance of these effects from above and below should be studied. The polar summer mesosphere is extremely cold such that ice particles form, resulting in Noctilucent Clouds and in particular electromagnetic wave scattering, manifest in Polar Mesosphere Summer Echoes. The polar stratosphere and troposphere are strongly affected by dynamic processes occurring in connection with the polar vortex. Röttger (1991) has initially summarized these research topics which can be studied by radar.

Mesosphere-stratosphere-troposphere (MST) radars contribute significantly to the studies of these processes. For this reason the Max-Planck-Institut für Aeronomie has established an MST VHF radar in Longyearbyen on Svalbard, the SOUSY Svalbard Radar (SSR). It is obvious that such MST radar studies are carried out in combination with other related observations, i.e. with the EISCAT Svalbard Radar (ESR) for mesospheric and D-region studies (Röttger and Tsuda, 1995), and with several in-situ and ground-based experiments performed by several research groups to study the Arctic mesosphere, stratosphere and troposphere. All these instruments, the radars, an OH spectrometer and an imaging riometer, are located close to Longyearbyen at 78• N, 16• E (Fig. 1).

In this paper we show initial results obtained with these two radars, the SSR and the ESR, to prove their capabilities for lower and middle atmosphere research without intending to present an exhaustive explanation yet. The presented interpretations of these first results are preliminary and not yet complete. Such extensions will follow in later papers.

2. The SOUSY Svalbard Radar

The SOUSY Svalbard Radar (SSR) of the Max-Planck-Institut für Aeronomie (MPAe) is an MST radar. It uses the main basic components of the mobile SOUSY radar and was installed near Longyearbyen in summer 1998. It consists of a transmitter operating on 53.5 MHz at a maximum peak power of 150 kW (6 kW average), a phased-array antenna consisting of 356 Yagi antennas (33 dBi gain and 4 degrees half-power beamwidth). Phase steering allows five beam-pointing directions at zenith and 5 degrees zenith angle to NE, SE, SW and NW. The transmitter, radar control, receiver and digital signal processing units and auxiliary equipment are housed in three containers. Fig. 2 shows the antenna array of the SSR at the end of Adventdalen/Bolterdalen. Several longer campaigns were performed in 1999 and further will follow in the coming two years. In the summer 2000 the antenna of the SSR is being separated into four receiving arrays to allow radar interferometer and imaging measurements.

SOUSY stands for SOUnding SYstem, which indicates that the SOUSY Svalbard Radar (Czechowsky et al., 1998) is used in a system of instruments to sound the atmosphere. Collaborations of the Max-Planck-Institut für Aeronomie, in charge of the SSR, with other research groups performing investigations on Svalbard are evolving and welcome.

3. The EISCAT Svalbard Radar

The EISCAT Svalbard Radar (ESR) is an incoherent scatter radar primarily designed for studies of the ionosphere (Röttger et al., 1995). It consists of a 1000 kW peak power transmitter (250 kW) operating at a center frequency of 500 MHz and a fully steerable parabolic dish antenna of 32 m diameter (42.5 dBi gain and a half-power beamwidth of 1.3•). Recently a fixed antenna of 42 m diameter was added, pointing in the direction of the Earth's magnetic field. The ESR has sophisticated modulation schemes, a multi-channel receiver, and a versatile radar controller as well as flexible signal processing instrumentation (Wannberg et al., 1997). It's capabilities for mesosphere and D-region research were summarized by Röttger et al. (1998). Experiment scheduling and operation of the ESR is according to rules decided by the EISCAT Scientific Association.

4. The Basic Scientific Objectives for Combined Radar Observations on Svalbard

The mesosphere can be studied with incoherent scatter, as well as with the MST (mesosphere-stratosphere-troposphere) coherent scatter radar technique. In the lower thermosphere and mesosphere the incoherent scatter process is collision dominated. Incoherent scatter measurements of the lower thermosphere and mesosphere allow the derivation of electron density, ion-neutral collision frequency (neutral density) and temperature, ion (neutral) velocity, ion composition and the density of negative and positive ions (e.g., Röttger, 1997). Such measurements are done with the EISCAT radars in Tromsø and on Svalbard. Occasionally, coherent scatter from ionization irregularities can mask the incoherent scatter measurements, particularly in summer when Polar Mesosphere Summer Echoes - PMSE - occur (Cho and Röttger, 1997).

Observations of the troposphere and the lower stratosphere are possible with ST (stratosphere-troposphere) radars, which are smaller versions of MST radars. These ST radars are also called wind profilers since they are also used in routine meteorological observations to measure continuously wind profiles and other meteorological parameters (Röttger and Larsen, 1990). ST radar wind profilers measure the vertical profile of the three-dimensional wind vector, atmospheric stability and turbulence intensity with height resolution of better than 100 meters and time resolution as good as several seconds. MST VHF radars can also be operated in the meteor radar mode with the required higher time resolution less than a few tens of milliseconds.

The radar scattering process is strongly dependent on the scales of ionospheric and atmospheric irregularities in the refractive index, i.e. on the applied radar wavelength. On radar wavelengths smaller than a meter, corresponding to the frequency 500 MHz used by the EISCAT Svalbard Radar, the turbulence scatter contribution to echoes from mesospheric altitudes is usually not detectable. The reason is that such radar wavelengths are much smaller than the scales of turbulence that can exist in the mesosphere. To operate the 500 MHz EISCAT Svalbard Radar as an MST radar for continuous studies of neutral mesospheric turbulence is therefore impossible. A

separate radar on a lower frequency such as 53.5 MHz is needed for that purpose. Simultaneous operation of a 53.5 MHz and a 500 MHz radar comprise a useful combination for mesospheric studies, since the former system is basically sensitive to mesospheric clear air turbulence, causing electron density irregularities, and the latter to ionospheric electron density. Also observations of Polar Mesosphere Summer Echoes - PMSE -, which are related to ice particles (Noctilucent Clouds - NLC -), are preferably done at lower frequencies (Cho et al., 1992), such as in the VHF band on 53.5 MHz. It had been expected and it was observed for the first time in summer 1999 that these particular echoes, which are not due to the common turbulence scatter, also occur occasionally at 500 MHz, which we will also discuss in this paper.

The SOUSY Svalbard Radar is applied to study the structure and dynamics of the lower and middle atmosphere. Possible auroral influences, solar proton events (SPE) and the resulting polar cap absorption phenomena (PCA) and their impact on middle atmosphere can be investigated in coordination with the EISCAT Svalbard Radar. The extent of Polar Mesosphere Summer Echoes (PMSE) and their relation to Polar Mesosphere Clouds (PMC) and Noctilucent Clouds (NLC) needs to be studied in higher Arctic latitudes, such as close to 80• on Svalbard. Klostermeyer (1997) developed a model to explain the PMSE, which should be tested by these radar observations. The winter absorption anomaly and its relation to stratospheric warming in the polar vortex and the corresponding planetary wave properties are not known at high latitudes of 80• . Most essential appears also the climatological study of winds, tides and long period waves and their non-linear interaction (Rüster, 1994) as well as particularly the climatology of atmospheric gravity waves in the polar lower and middle atmosphere (Yoshiki and Sato, 2000), the supposed acceleration of the mean wind by momentum deposition by gravity waves and the effect on the middle atmosphere temperature. Such processes are principally illustrated in Fig. 3. We note that the combination of MST radar, covering the middle and lower atmosphere, and the incoherent scatter radar, covering the region above, is a highly useful endeavor. Thomas (1996) had postulated possibilities that PMSE are sensitive early indicators of global change due to mesospheric temperature and water vapor changes. To follow this up, long-term observations of PMSE are required.

McIntyre (1999) has summarized the current understanding of the dynamics of the middle atmosphere and highlighted open questions. We believe that MST radars, operated in high latitudes, can well contribute to foster the further understanding of dynamical processes governing the middle atmosphere.

5. The Mesosphere as Studied by Incoherent Scatter and MST Radar

Particular phenomena in the polar atmosphere and the auroral ionosphere, namely particle precipitation, Joule heating, electric fields and Lorentz forcing as well as vertical transport of constituents and momentum, which result from magnetosphere-ionosphere coupling, have an impact on the middle atmosphere, where they can be studied by radar (Röttger, 1994). Furthermore dynamic processes, such as tides (Aso et al., 1999) and gravity waves and their interactions (Rüster, 1994), which originate in the lower atmosphere (troposphere) and the middle atmosphere (stratosphere and mesosphere), propagate upwards into the thermosphere. These mutual coupling processes, which affect the structure, dynamics and aeronomy of the middle atmosphere and lower thermosphere, take place uniquely in the high latitude mesosphere, where the effects from the magnetosphere and ionosphere merge with the effects from the lower and middle atmosphere.

Mesosphere/D-region investigations should be carried out by combined operation of the EISCAT Svalbard Radar and the SOUSY Svalbard Radar, such as studies of the impact of precipitating electrons and protons on D-region electron density, and of changes in composition and their effects on Polar Mesosphere Summer Echoes. How these coupling processes between the magnetosphere and the ionosphere, the thermosphere and the middle atmosphere take place in the high polar region is so far fairly unknown, since appropriate radar instruments had not been operated at the latitudes near 80• . For instance, the influx of solar protons into the polar mesosphere and upper stratosphere evidently has an influence on the ozone budget (Stephenson and Scourfield, 1992). Solar proton events (leading to polar cap absorption) can be studied by the EISCAT Svalbard Radar, the SOUSY Svalbard Radar and imaging riometers. It would also be useful to allow simultaneous radar experiments in the auroral zone (EISCAT Tromsø (Röttger, 1997), in Andoya (Singer et al., 1996), and Kiruna (Kirkwood et al., 1998)) and in the Arctic on Svalbard, using the radars described in this paper, to study the meridional variation of these effects and their occurrences. The addition of the imaging riometer IRIS in Longyearbyen (Stauning, 1996) and Nyålesund (Nishino, 1997) will be most valuable for these purposes. The latitudinal variation of PMSE is being studied by comparing observations with the SSR at 78• N and the ALOMAR VHF radar ALWIN at 68• N (Singer et al., 1999), which are both at the same longitude.

The SSR is also capable of detecting meteor echoes. These can be used to determine wind velocities and temperatures in the upper mesosphere and lower thermosphere (Hocking et al., 1997). A combination with concurrent temperature measurements with the OH spectrometer located at the Auroral Observatory (Fig. 1) is most useful (Nielsen et al., 2000). Independently of applying the SSR for occasional meteor observations, a separate continuously operating meteor radar will be highly valuable for studies of tides and mean winds.

6. The Arctic Stratosphere and Troposphere as studied by MST Radar

There are certain phenomena in the polar middle and lower atmosphere which need to be studied by radar, in addition to the multitude of other experiments which are already applied for these studies in the Arctic and Antarctic. These are particularly those directed to the ozone variation, which is affected by dynamical processes related to the polar vortex (e.g., Sobel et al., 1997). We will discuss only those phenomena that can be investigated with an ST radar (stratosphere-troposphere radar). These are the structure and dynamics of the troposphere and the lower stratosphere in the polar region (see Fig. 3).

With ST radars and wind profilers it is possible to study dynamic processes in a wide scale range from planetary and synoptic scale disturbances to small-scale gravity waves and clear air turbulence. The wind field variations occurring in the polar vortex can be monitored continuously by ST radar wind profiler, although at one location and up to about 15-25 kilometers height. In polar regions it is of special interest to investigate with radar the exchange processes between the troposphere and the lower stratosphere, namely the variation of the tropopause height and the dynamics of tropopause folds (e.g., Elbern et al., 1998). The possibility to study vertical transport between the troposphere and the stratosphere, and the transport within the stratosphere by means of the mean vertical motion and by turbulent diffusion, is challenging (Ebel et al., 1991). The transport and deposition of energy and momentum by gravity waves in the lower stratosphere, which can be measured with ST radar (Worthington and Thomas, 1996), has an impact on the mean stratospheric circulation and the polar stratosphere temperature. Furthermore, polar stratospheric clouds, which are related to mountain and lee waves, have control of ozone depletion (e.g., Tie et al., 1996). The formation of mountain waves can be studied by ST radar (Röttger, 2000) and thus the dynamics below, and possibly in and around polar stratospheric clouds can also be investigated by the SOUSY Svalbard Radar. This ST radar, when it will be operated continuously in the wind profiler mode, would also yield invaluable input data for meteorological modeling and forecasting (Lafaysse, 1994).

Such operations of the SSR can most effectively contribute to research programs for studies of the Arctic troposphere and stratosphere being performed in Longyearbyen and Nyålesund on Svalbard.

7. Initial Observations of the Troposphere and Stratosphere with the SOUSY Svalbard Radar (SSR)

The SSR has proved its capabilities for proper observations of the mesosphere, stratosphere and troposphere during initial operations done in September 1998, in a continuous PMSE campaign between 10 June and 28 August 1999 and a special campaign for Leonid meteor observations in November 1999. Two stratosphere-troposphere operations over four days each were carried out at the end of August and in November 1999. The following results from these first operations are preliminary and should just prove the capabilities of the SSR for relevant scientific research. More

I 06

detailed analyses and explicit interpretations are following separately.

An example of initial tropospheric and lower stratospheric observations with the SOUSY Svalbard Radar is shown in Fig. 4. It displays the first height-time-intensity plot, and estimates of signal amplitude, which was recorded during a system test on 8 September 1998. This record covers 32 seconds; the antenna pointed vertically and the peak transmitter power was 120 kW, applying a hybrid operating mode consisting of single pulse and an 8-bit complementary code with 2 us baud length, corresponding to 300 m range resolution. Thin layers of increased echo strength are noticed up to altitudes above 20 km. The height profile of amplitude shows enhancements around 8 km and 13 km, which are attributed to inversion layers. The enhancement at 14 km is a consistent indicator of the tropopause (Röttger and Larsen, 1990). Whereas this system set-up was used in 1998, we implemented another version for stratosphere-troposphere observations in 1999, which used only 4 Yagi antennas for reception and 60 kW peak power in order to allow lower altitudes to be examined, too.

The capability of the SSR to point the antenna beam into five directions allows the deduction of estimates of the horizontal and the vertical velocity components. In our first attempts to test the capabilities of the SSR for the stratosphere-troposphere observations we have not removed the effect of anisotropy or layer tilts when deducing these velocity estimates. This analysis, taking into account all precautions and calibrations due to aspect sensitivity etc. (Röttger and Larsen, 1990), will be done in later phases.

In Fig. 5 we show 20 minute average profiles of the velocity components together with the power profile. The latter, taken with vertical antenna beam, proves that signals up to about 25 km can be detected. The distinct power enhancement at 13 km indicates the tropopause. All three velocity components show wavelike variations as a function of altitude, which can still be detected in the lower stratosphere. The variations of the horizontal velocity are approximately in phase in the upper troposphere and lower stratosphere, which is consistent with a standing wave. We assume that this is due to a mountain lee wave, which propagated into the lower stratosphere (Röttger, 2000).

Such lee waves seem to be characteristic for Svalbard. This is not unexpected due to the profile of this archipelago, where mountains steeply rise from sea level up to some 1000 m altitude and which is some 1000 km away from the next adjacent territory. We notice such wave structures in several of our troposphere-stratosphere observations. Fig. 6 shows height-time-intensity plots of radar reflectivity and radial velocity measured with vertical beam, recorded over 18 hours. The latter is an initial estimate of vertical velocity. We observe that the vertical velocity changes sign as function of altitude. The most intriguing observation is that this reversal of the velocity direction changes also as function of time. This needs more detailed analyses, including the horizontal wind, the aspect sensitivity and the tilt of reflectivity structures. The lower panel of Fig. 6 shows the corresponding reflectivity changes over time. We also notice the enhancement at the tropopause, which is at fairly high altitude of about 13-14 km and split into multiple inversions.

Fig. 7 shows that such lee wave structures do not occur all the time. Indeed, the velocity (upper panel of Fig. 7) indicates clear signs of shorter period oscillations, which we attribute to

I 07

propagating short period gravity waves. The velocity amplitudes are much smaller than those during the lee wave events. The dominating period increases from about 10 minutes to some 30 minutes at the end of the displayed period. We again need to analyze more measured parameters to understand this variation. The reflectivity plot (lower panel of Fig. 7) indicates a low tropopause at 8-9 km in the beginning, which moved to about 12 km at the end of the period. After 14-15 UT downward moving structures detached from the tropopause. This is obviously a sign of a warmfront passage (Röttger and Larsen, 1990). We do not note a clear tropopause break but a separation into more than three substructures of the corresponding warm front. The passage of a warm front was clearly seen in the weather maps, but not the split into substructures. When the front passed the surface, the temperature increased rapidly. Again, we need to analyze this event in more detail in future. For this purpose we have got the weather maps from the Norwegian Flight Weather Service, Longyearbyen, and the radiosonde data from Nyålesund (Alfred-Wegener-Institut), which is about 100 km north of the SSR.

It will be a major challenge to investigate further details of these new observations, which should shed more light into the structure and dynamics of the Arctic troposphere and stratosphere over Svalbard. The results shown in Figs. 6 and 7 were obtained with a simple receiving antenna of 4 Yagis only, which had to be used due to transmit-receive switching problems affecting the lower altitude records. We are designing a modification that will allow more receiving antennas and rise the sensitivity by 16 dB. This will provide complete data coverage throughout the troposphere and the lower stratosphere up to about 20 km and also adds spaced antenna radar interferometry and imaging capabilities to the SSR.

8. Some Initial Mesosphere Observations with the SOUSY Svalbard Radar (SSR) and the EISCAT Svalbard Radar (ESR)

The SOUSY Svalbard Radar (SSR) was particularly designed for observations of Polar Mesosphere Summer Echoes - PMSE - (Czechowsky et al. 1998). After some repair, following unusual snowdrift problems, the operation for PMSE observations was started on 10 June 1999 and continued uninterruptedly until 28 August 1999, when the troposphere-stratosphere operation, described in the former chapter, did commence. Between 10 July and 15 July 1999 the EISCAT Svalbard Radar (ESR) was operated in a specially designed mode to detect PMSE and compare these with those observed with the SSR. An initial version of this code was applied at the ESR for D-region incoherent scatter observations in April 1998.

The SSR was run at 60 kW with 4% duty cycle. A 20-bit complementary code was applied. The range sampling was at 2 μs (300 m range resolution) and the interpulse period was 1 ms. The antenna was sequentially pointed into five directions: the zenith and at five degrees off-zenith to NE, SE, SW and NW. The dwell time in each direction was 6 s when 64 coherently integrated samples were taken at ranges between 72 km and 120 km at 300 m range resolution. The Nyquist frequency resulting from the coherent integration time is • 5.6 Hz, resulting in a maximum un-aliased radial velocity of • 15.75 m s^{-1}. The data were decoded on-line and stored in binary format on disk cartridge or tape. After ASCII conversion of the original binary data and copy on CD-ROM

the data were analyzed off-line.

Rather than using the standard so-called 'gup' routines of the ESR (Wannberg et al., 1997), which are not too suitable for D-region and PMSE studies, a special program was designed for the ESR using a 32-bit complementary code, a variety of range gate widths and numbers, and adapted interpulse periods to match the conditions of incoherent scatter and coherent scatter from PMSE (Röttger et al., 1998). Most of the data were taken using an interpulse period of 1.35 ms. These raw data were stored on disk after on-line decoding. The analysis took into account the removal of the strong ground clutter, where the standard method applied in the MST radar technique could be used, since the clutter has a much narrower frequency bandwidth than the ionospheric signal. The groundclutter width usually is less than 0.1 Hz, which compares to minimum signal bandwidths of a few Hz. The 2.7 ms sampling time (resulting from the complementary code) corresponds to a Nyquist frequency of • 185 Hz, which is sufficient for coherent scatter from PMSE (occurring in the altitude range 80-90 km) and for incoherent scatter up to about 88 km. The maximum unaliased velocity is • 55.5 m s^{-1}. The ESR was operated at full peak power close to 1000 kW and an average power between 9% and 22%, depending on range resolution (between 600 m and 1500 m). The antenna was pointed to several directions close to zenith. The data, originally available in the EISCAT MATLAB-format, were converted into ASCII and dumped on tape and CD-ROM for off-line analysis.

Fig. 8 shows an example of PMSE recorded with the SOUSY Svalbard Radar on 27 June 1999. We have selected the vertical antenna beam for these displays. The upper panel shows the height-time-intensity (HTI) diagram and the lower seven panels show the dynamic spectra for the range gates embraced by the red lines in the HTI diagram. The PMSE are frequently characterized by very structured layering, which often split into two sheets. Occasionally these split further into thinner laminae. This feature seems to be more pronounced in our observations as compared to lower latitudes (e.g. 10• further south over northern Scandinavia, Bremer et al., 1996). These structures have a tendency to move downwards and are additionally modulated by wavelike oscillations. This is consistent with earlier observations (see review by Cho and Röttger, 1997). The dynamic spectra show quasi-periodic variations of the mean velocity, which reaches amplitudes of 7.5 m s^{-1}. Between 09 and 10 UT these variations are highly periodic but triangle-shaped, which is a new observation indicating some non-linearity. We also notice the velocity jumps around 12:30 UT, somewhat similar as earlier observed with the EISCAT VHF radar in Tromsø (Röttger, 1994).

In July 1999 the first simultaneous operation of the SSR and the ESR were performed, since it was estimated that PMSE should occasionally also be observed on 500 MHz. The unique possibility of comparing spectral features and scatter cross sections in the common volume observed simultaneously on 53.5 MHz (SSR) and 500 MHz (ESR) was exciting. Echoes were only observed much less frequent on 500 MHz than on 53.5 MHz. Fig. 9 shows an example of an HTI diagram and dynamic spectra of PMSE detected with the ESR on 15 July 1999. The burst-like occurrence of very wide spectra indicating violent turbulence of some 20 m s^{-1} rms velocity variations is very striking. Below this violent turbulence regime an extremely stable stratification occurred characterized by a very narrow spectrum. Fig. 10 shows the concurrent PMSE observations with the SSR, which also exhibit broad and narrow spectra during this event. Most likely, the larger beamwidth of the SSR (4 degrees) as compared to the ESR (1.23 degrees beam

width) resulted in stronger beamwidth broadening of the 53.5 MHz echoes. Absolute scatter cross sections of PMSE can be calculated for the ESR and SSR. The corresponding radar reflectivities (cross section per unit volume) are in the order of 10^{-14} - 10^{-15} m^{-1} for the SSR and 10^{-19} - 10^{-20} m^{-1} for the ESR. We can also estimate the turbulence dissipation rate from the spectral widths and the electron density (profile) from the ESR. Using the model of Cho et al. (1992) we then can determine the Schmidt number. An initial estimate from our comparisons yields Schmidt numbers larger than 100. Using this combination of ESR (500 MHz) and SSR (53.5 MHz) seems to be a proper tool to obtain such an estimate from radar observations.

As surmised in earlier interpretations of PMSE we deduce from our initial observations on 53.5 MHz and 500 MHz that the irregularities responsible for the PMSE occur mostly in fairly persistent sheets and layers, which are just perturbed by neutral turbulence. Further consideration of this hypothesis will be treated in subsequent analyses. This will also take into account theoretical developments of Klostermeyer (1997). We assume that the low occurrence of PMSE on 500 MHz was partially caused by very low D-region ionization. The increase of background echo intensity (which is due to incoherent scatter) observed above about 90 km in Fig. 9 shows that there was very little ionization below this altitude. All our observations with the ESR were during such ionospherically quiet periods, when enhancements due to particle precipitation did not occur (according to the collocated observations with the imaging riometer IRIS; personal communication by Stauning, 1999). We do not exclude, however, that also the temperature structure was not an optimum for PMSE during this short observing period. This needs to be studied further.

The PMSE operating campaign of the SSR took place over more than eighty days in summer 1999. This long time series allows to study longer period variations due to tides and planetary waves and their non-linear interaction (Rüster, 1994). The analysis of this long period will also include comparisons with imaging riometer to investigate the dependence on D-region ionization. We will also compare the PMSE occurrence and tidal and planetary wave features with those observed at other observatories, such as Andoya, Kiruna and Resolute Bay.

During intensified D-region ionization the ESR is capable of detecting incoherent scatter echoes from altitudes down to some 55 km. This is shown in Fig. 11. This record was obtained at the end of a larger polar cap absorption event, which had lasted over a few days as recorded by the riometer in Nyålesund (Nishino, 1997). This will allow profiles of electron density, negative ions and velocities and possibly temperature to be measured throughout the mesosphere. Further details have to be investigated in due course.

9. Meteor Observations with the SOUSY Svalbard Radar

Although the SSR was not originally conceived of or optimized for operation as meteor radar, it detects meteors like every MST radar does. This feature can be used to obtain wind and temperature estimates, and some information about the meteorites impinging into the lower thermosphere and upper mesosphere. Around the Leonid meteor shower in November 1999 the SSR was operated in a special meteor radar mode with a short coherent integration time of less than 30 ms and antenna beam directions fixed for longer periods (usually 1 hour per direction). We have

collected more than 4 days of meteor data and noticed that the occurrence rate of meteor echoes during the maximum of the Leonid shower around 01-03 UT on 18 November 1999 was about three times as high as compared to normal times.

Fig. 12a shows a long-lasting meteor echo of particular nature. At 21:55:04 UT we notice a thin echo streak moving from 105 km to 85 km within a small fraction of a second. The target must have come down through the radar beam with a velocity of some 60 km s^{-1}. We therefore attribute this echo to come from the meteorite head. Subsequently the trail, likely generated outside the main radar beam, drifted through it by the mean wind.

Fig. 12b shows an example of a long lasting, subjectively termed, underdense meteor echo observed between 02:56:03 and 02:56:12 UT, the peak of the Leonid shower, on 18 November 1999 at altitudes of about 90 km and 115 km. The decay of the echo is partially due to the meteor trail carried through the antenna beam by the mean wind and partly by its diffusion. Deducing the former from the measured Doppler shift, it is possible to use the decay time of this long-lasting echo to estimate the diffusion coefficient and hence the temperature profile (e.g., Hocking et al., 1997). The latter method preferably should be applied by selecting many of the short-lived underdense echoes that were observed during our campaign. The temperature estimates are being compared with simultaneously deduced temperature estimates with the OH spectrometer operated at the Auroral Observatory (Nielsen et al., 2000). Initial comparisons show a promisingly fair agreement.

These preliminary observations prove that useful information can be extracted from the meteor observations of the SSR. We are convinced, however, that a special purpose meteor radar with wider beam and receiving interferometry would be an advisable improvement for such observations.

10. Summary and Outlook

We have shown the new capabilities of the SOUSY Svalbard Radar for scientific research of the polar atmosphere. Its combination with the EISCAT Svalbard Radar is most useful for PMSE studies and in particular also for measuring background electron density profile during such events. Due to the unfavorable geophysical conditions during our initial campaign in July 1999, the latter was not fully possible yet. This should be attempted again in the coming years.

Major new findings are also expected by operating the SSR for troposphere and stratosphere research. We have shown a few impressive examples of such ST records. In particular, we expect another major step forward after implementation of multiple receiving antennas for radar interferometry and imaging, which will be done in summer 2000.

The Max-Planck-Institut für Aeronomie (MPAe) has installed the SOUSY Svalbard Radar on site in summer 1998, started successful tests soon thereafter and performed long campaign operations in 1999. Collaborations with other research groups should be established more formal in future, in particular with those institutions performing complementary observations on Svalbard. An initial one was a campaign carried out in cooperation with the University Courses on Svalbard

(UNIS). This campaign was called UNILEO, stemming from the collaboration with UNIS during the Leonid meteor shower.

We are planning subsequent scientific campaign and regular routine operations, which should be introduced in later phases of this project. Close scientific collaborations are now being discussed and examined with EISCAT, UNIS, University in Tromsø in Norway, the Alfred-Wegener-Institut für Polar- und Meeresforschung (AWI) in Germany and the National Institute of Polar Research (NIPR) in Japan. Agreements have been signed with the Alfred-Wegener-Institut for common observations during the ASTAR 2000 campaign (Arctic Study of Tropospheric Aerosol and Radiation) in March and April 2000, and with the Leibniz-Institut für Atmosphärenphysik for coordinated observations of the mesosphere during the ROMA campaign (Rocket-borne Observations in the Middle Atmosphere) in July to September 2000. Further collaborations are welcome.

Acknowledgement:

The most helpful support by the Governor's office, many institutions, administrations, companies and individuals in Longyearbyen, Tromsø and Oslo, which was substantial for the successful installation of the SOUSY Svalbard Radar project is highly appreciated. My thanks are directed to my colleagues of the SOUSY scientific group at the Max-Planck-Institut für Aeronomie, P. Czechowsky, J. Klostermeyer, R. Rüster and G. Schmidt, for their useful collaboration and to the MPAe Director emeritus, T. Hagfors, for supporting this project. In particular I like to address my thanks and recognition to the engineering and technical group of the Max-Planck-Institut under K. Meyer, K.D. Preschel, H. Becker and J. Trautner as well as many others at MPAe for their efforts and support in constructing and operating the SOUSY Svalbard Radar. The collaborations with J. Markannen of EISCAT in performing the ESR experiments and C. Hall of the University in Tromsø are well appreciated. I also thank T. Aso of NIPR inviting and encouraging me to prepare this paper. The SOUSY Svalbard Radar is a project of the Max-Planck-Institut für Aeronomie. The EISCAT Svalbard Radar is operated and funded by CNRS (France), MPG (Germany), NFR (Norway), NRF (Sweden), NIPR (Japan), PPARC (UK) and SA (Finland). The author thanks anonymous referees for their kind comments in reviewing this paper.

References:

Aso, T., van Eyken, A., and P.J.S. Williams (1999): EISCAT Svalbard Radar-derived atmospheric tidal features in the lower thermosphere as compared with the numerical modeling ATM2, **Adv. Polar Upper Atmosph. Res., 13**, 48-56.

Bremer, J., P. Hoffmann, A.H. Manson, C.E. Meek, R. Rüster, and W. Singer (1996): PMSE observations at three different frequencies in northern Europe during summer 1994, **Ann. Geophys., 104**, 1317-1327.

Cho, J.Y.N., T.M. Hall, and M.C. Kelley (1992): On the role of charged aerosols in Polar Mesosphere Summer Echoes, **J. Geophys. Res., 97**, 875-886.

Cho, Y.N., and J. Röttger (1997): An update review of polar mesosphere summer echoes: Observations, theory, and their relationship to noctilucent clouds and subvisible aerosols, **J. Geophys. Res., 102**, 2001-2020.

Czechowsky, P., G. Schmidt, and R. Rüster (1984): The mobile SOUSY Doppler radar: Technical design and first results, **Radio Sci., 19**, 441-450.

Czechowsky, P., J. Klostermeyer, J. Röttger, R. Rüster, and G. Schmidt (1998): The SOUSY-Svalbard-Radar for middle and lower atmosphere research in polar regions, **Proc. 8th Workshop on Techn. Sci. Aspects of MST Radar**, SCOSTEP, 318-321.

Ebel, A., H. Hass, H.J. Jakobs, M. Laube, M. Memmesheimer, A. Oberreuter, H. Geiss, and Y.H. Kuo (1991): Simulation of ozone intrusion caused by a tropopause fold and cut-off low, **Atmos. Env., 25A**, 2131-2144.

Elbern, H., J. Hendricks, and A. Ebel (1998): A climotology of tropopause folds by global analyses, **Theor. Appl. Climatol., 59**, 181-200.

Hall, C.M., and T. Aso, mesospheric velocities and buoyancy subrange spectral slopes determined over Svalbard by ESR (1999): **Geophys. Res. Lett., 26**, 1685-1688.

Hocking, W.K., T. Thayaparan and J. Jones (1997): Meteor Decay Times and their Use in Determining a Diagnostic Mesospheric Temperature-Pressure Parameter: Methodology and One Year of Data, **Geophys. Res. Lett.**, 24,23, 2977-2980.

Kirkwood, S., V. Barabash, P. Chilson, A. Rechou, and K. Stebel (1998): The PMSE season -its relation to wind, temperature, and water vapor, **Geophys. Res. Lett., 25**, 1867-1879.

Klostermeyer, J. (1997): A height- and time-dependent model of polar mesosphere summer echoes, **J. Geophys. Res., 102**, 6715-6727.

Lafaysse, C. ed. (1994): Utilization of UHF/VHF radar wind profiler networks for improving

weather forecasting in Europe, **COST 74** Final Report, European Commission, Brussels.

McIntyre, M.E. (1999): How far have we come in understanding the dynamics of the middle atmosphere?, Proc. 14th ESA-PAC Symposium, **ESA SP-437**, 581-590.

Nielsen, K.P., Röttger, J., and F. Sigernes (2000): Simultaneous measurements of temperature in the upper mesosphere with a VHF meteor radar and OH spectrometer from Svalbard, manuscript in preparation.

Nishino, M., H. Yamagishi, P. Stauning, T.J. Rosenberg, and J.A. Holtet (1997): Location, spatial scale and motion of radio wave absorption in the cusp-latitude ionosphere observed by imaging riometers, **J. Atmos. Terr. Phys., 59,8**, 903-924.

Röttger, J., J. Klostermeyer, P. Czechowsky, R. Rüster, and G. Schmidt (1978): Remote Sensing of the Atmosphere by VHF Radar Experiments, **Naturwissenschaften, 65**, 285-196.

Röttger, J., and M.F. Larsen (1990): UHF/VHF Radar Techniques for Atmospheric Research and Wind profiler Applications, in **Radar in Meteorology**, American Meteorological Society, 235-281.

Röttger, J. (1991): MST Radar and Incoherent Scatter Radar Contributions to Studying the Middle Atmosphere, **J. Geomagn. Geoelectr., 43**, 563-596.

Röttger, J. (1994): Middle Atmosphere and Lower Thermosphere Processes at High Latitudes studied with the EISCAT Radars, **J. Atmos. Terr. Phys., 56**, 1173-1195.

Röttger, J. (2000), ST radar observations of atmospheric waves over mountainous areas: A review, **Ann. Geophys., 18**, in print.

Röttger, J., and T. Tsuda (1995): Studies of the Polar Middle and Lower Atmosphere by an MST Radar on Svalbard, **J. Geomagn. Geoelectr., 47**, 929-942.

Röttger, J. (1997): Radar observations of the middle and lower atmosphere, in Incoherent Scatter Theory, Practice and Science, D. Alcayde, ed., **Techn. Report 97/53**, EISCAT Scientific Association, 263-314.

Röttger, J., J. Markannen, and U.G. Wannberg (1998): The EISCAT Svalbard Radar - Its potential for middle atmosphere studies, **Proc. 8th Workshop on Techn. Sci. Aspects of MST Radar**, SCOSTEP, 314-317.

Rüster, R. (1994): VHF radar observations of non-linear interactions in the summer polar mesosphere, **J. Atmos. Terr. Phys., 56**, 1289-1299.

Singer, W., D. Keuer, P. Hoffmann, P. Czechowsky and G. Schmidt (1996): The ALOMAR SOUSY Radar: Technical Design and Further Developments, **Proc. 7th Workshop on Techn. Sci. Aspects of MST Radar**, SCOSTEP, 473-476.

I 14

Sobal, A.H., R.A. Plumb, and D.W. Waug (1997): Methods of calculating transport across the polar vortex, **J. atmos. Sci., 54**, 2241-2260.

Stauning, P. (1996): Investigations of ionospheric radio wave absorption processes using imaging riometer techniques, **J. Atmos. Terr. Phys., 58**, 753-764.

Stephenson, J.A.E., and W.J. Scourfield (1992): Ozone depletion over the polar caps caused by solar protons, **Geophys. Res. Lett., 12**, 2425-2428.

Thomas, G.E. (1996): Global change in the mesosphere-lower thermosphere region: has it already arrived?, **J. Atmos. Terr. Phys., 58**, 1629-1656.

Tie, X., G.P. Brasseur, C. Granier, A. De Rudder, and N. Larsen (1996): Model study of polar stratospheric clouds and their effect on stratospheric ozone, 2. model results, **J. Geophys. Res., 101**, 12575-12584.

Wannberg, G., I. Wolf, L.G. Vanhainen, K. Koskeniemi, J. Röttger, M. Postila, J. Markannen, R. Jacobsen, A. Stenberg, R. Larsen, S. Eliassen, S. Heck and A. Huuskonen (1997): The EISCAT Svalbard Radar: A case study in modern incoherent scatter radar design, **Radio Sci., 32,6**, 2283-2307.

Worthington, R.M., and L. Thomas (1996): The measurement of gravity wave momentum flux in the lower atmosphere using VHF radar, **Radio Sci., 31**, 1501-1517.

Yoshiki, M., and K. Sato (2000): A statistical study of gravity waves in the polar regions based on operational radiosonde data, **J. Geophys. Res.**, revised.

TR

Figure Captions:

Fig. 1 The locations of facilities for middle and upper atmosphere research in the vicinity of Longyearbyen Svalbard. The EISCAT Svalbard Radar (ESR) is close to the top and the SOUSY Svalbard Radar (SSR) at the foot of the mountain of coalmine 7. The imaging riometer (IRIS) is close to the Auroral Observatory, where also the OH spectrometer is located.

Fig. 2 Part of the antenna array of the SOUSY Svalbard Radar in Advent-dalen/Bolterdalen near Longyearbyen.

Fig. 3 Processes in the polar mesosphere, stratosphere and troposphere, which can be studied by an MST VHF radar (SSR). The lower thermospheric and ionospheric processes are measured by incoherent scatter radar (ESR); from Röttger and Tsuda (1995).

Fig. 4 Quicklook example of first SSR measurements of the troposphere and stratosphere using the full antenna for transmission and reception. Left-hand: Height-time-intensity plot, covering a short period of 32 seconds, showing thin layers in the troposphere and lower stratosphere. Right-hand: Scatter plot of normalized power P (signal + noise). The antenna was pointing into vertical direction.

Fig. 5 Height profiles of signal power P (normalized to the noise level at 0 dB), radial velocity in the vertical beam (W), and zonal (U) and meridional (V) wind velocity, measured with the SSR on 4 September 1998 at 15:57-16:18 UT.

Fig. 6 Height-time-intensity plots of received normalized power P (lower panel) and radial velocity W' in the vertical beam direction (upper panel), recorded with the SSR between 07:39:18 UT on 14 November 1999 and 01:35:05 UT on 15 November 1999. The velocity scale is between -1 m s^{-1} (black) and +1 m s^{-1} (magenta); velocity estimates are affected by noise below and above the tropopause. The power is normalized to the noise level and its scale is between 0 dB (noise level; yellow) and 20 dB (magenta). Transmission was with the full 356-Yagi antenna and reception was with 4 Yagis only.

Fig. 7 Same as Fig. 6, but between 11:00:38 UT on 13 November 1999 and 04:56:24 UT on 14 November 1999.

Fig. 8 Polar Mesosphere Summer Echoes recorded with the SSR (vertical beam) between 07:45:03 UT and 13:05:25 UT on 27 June 1999. The upper panel shows the height-time-intensity plot between 79.2 km and 95.7 km altitude, and the lower 7 panels the dynamic spectra of altitude gates 83.7 km and 85.5 km. The Doppler frequency limits in this display are • 2.8 Hz, corresponding to a radial velocity of • 7.9 m s^{-1}. The center red line indicates zero velocity.

Fig. 9 Polar Mesosphere Summer Echoes recorded with the ESR (antenna pointing 30• degrees zenith angle at 135• azimuth) on 15 July 1999. The upper panel shows the height-time-intensity plot between 78.3 km and 101.7 km altitude. The lower six panels show the dynamic

T17

spectra for the range gates between 85.2 km and 89.7 km. The Doppler velocity limits in this display are • 27.8 m s^{-1}; zero velocity is indicated by the red line.

Fig. 10 Same as Fig. 8 but dynamic spectra between 85.2 km and 89.7 km with different time-scale to match to the time scale of Fig. 9, which was recorded simultaneously with the ESR on 15 July 1999.

Fig. 11 Incoherent scatter echoes observed with the ESR on 24 April 1998 between 11:15 UT and 11:45 UT with antenna beam pointing into direction of the Earth's magnetic field. The Doppler velocity limits are • 55.5 m s^{-1}; the tick marks on the height axis and the red lines in the right-hand panel correspond to zero Doppler velocity in the corresponding range gate. The left-hand panel shows the dynamic spectra and the right-hand panel the distributions of relative power during the observing period.

Fig. 12a Meteor echo detected with the SSR on 9 November 1999 between 21:55:04 and 21:55:10 UT with the antenna beam pointing at 5• zenith angle into SW direction.

Fig. 12b Meteor echo detected with the SSR on 18 November 1999 between 02:56:03 and 02:56:12 UT on 18 November 1999 with the antenna beam pointing at 5• zenith angle into NW direction.

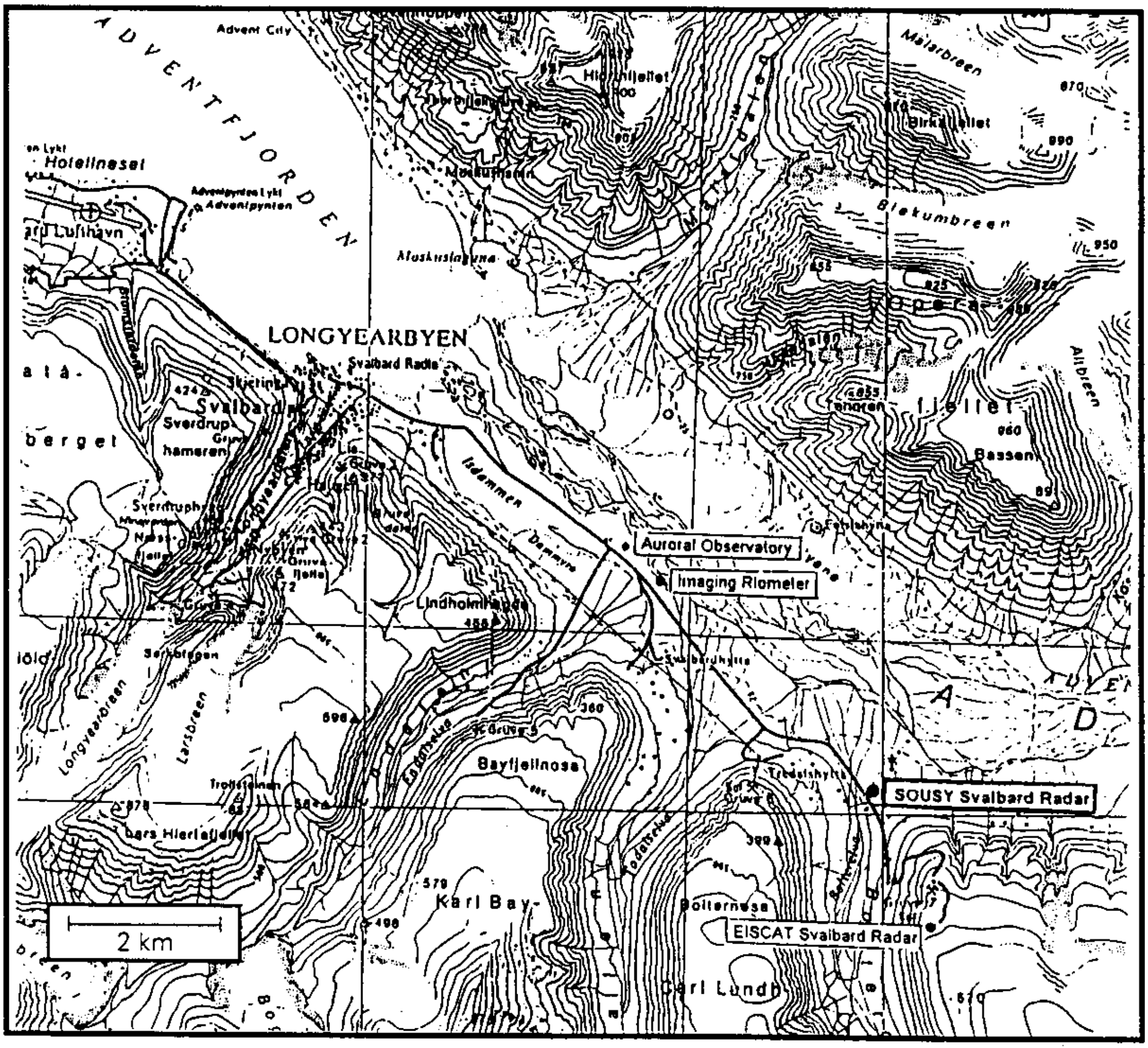
ADVENTFJORDEN
Advent City
Hotellneset
Adventpynten
LONGYEARBYEN
Svalbard Radio
Sverdrup
hameren
Hiorthfjellet
Blekumbreen
Birkafjellet
Bassen
Isdammen
Auroral Observatory
Imaging Riometer
Lindholmhøgda
Bayfjellnosa
Longyearbreen
Larsbreen
Lars Hierta fjellet
Karl Bay
Bolternosa
Carl Lundh
SOUSY Svalbard Radar
EISCAT Svalbard Radar
2 km

Fig. 1

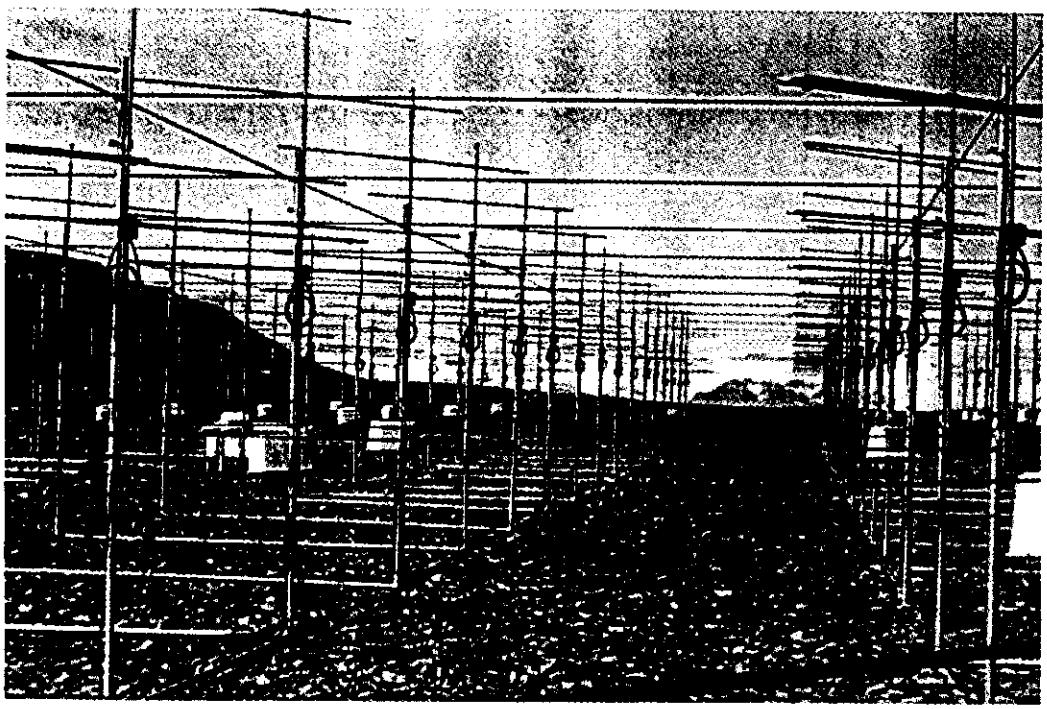

The **SOUSY-Svalbard-Radar**
located near Longyearbyen(78°N, 16°E)
operated by the Max-Planck-Institut für Aeronomie
is used for studies of the structure and dynamics of the polar atmosphere.
The photo shows part of the antenna array, consisting of 356 Yagi elements.
The operating frequency is 53.5 MHz and the peak power 60 (150) kW

Fig. 2

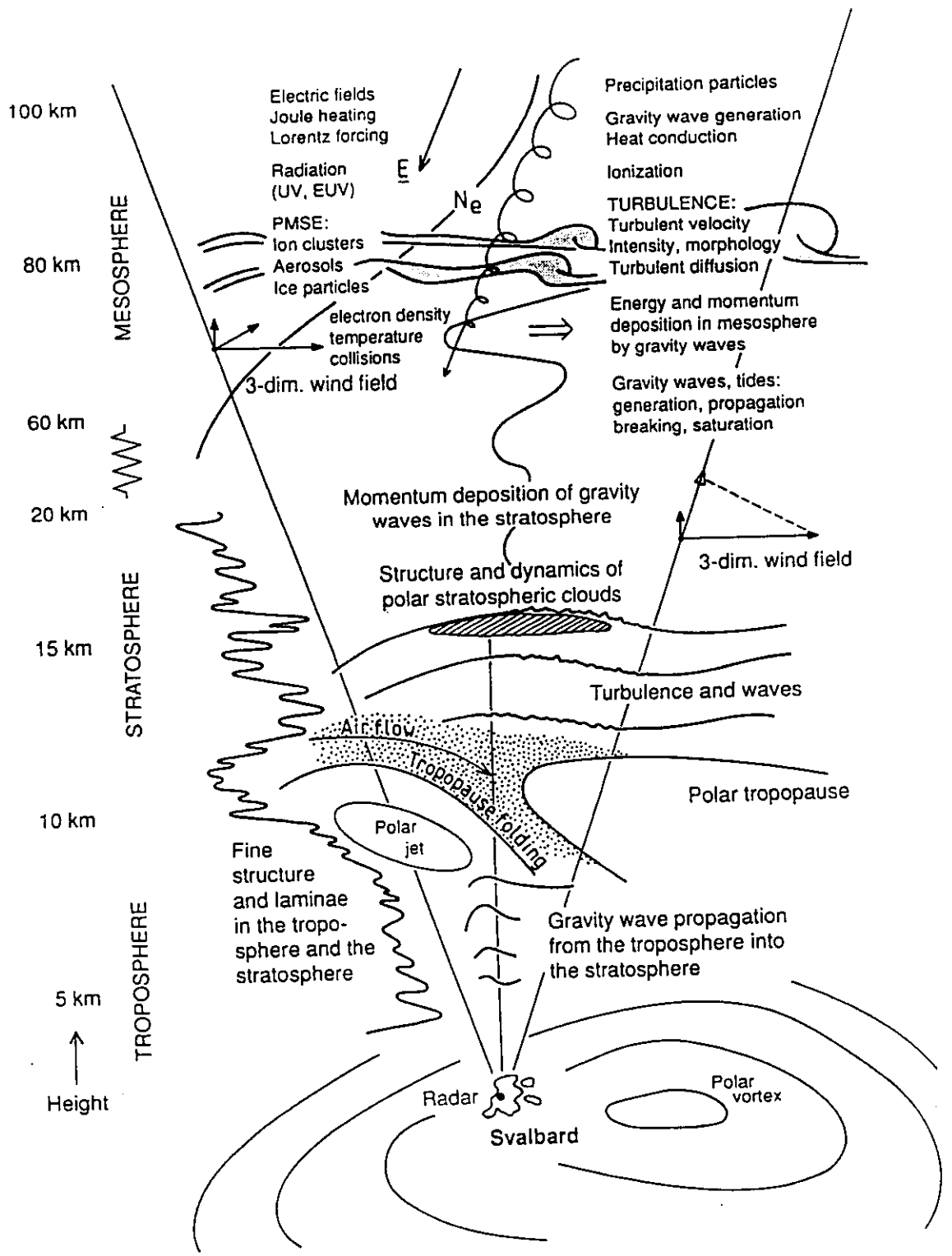
100 km
80 km
60 km
20 km
15 km
10 km
5 km
Height
MESOSPHERE
STRATOSPHERE
TROPOSPHERE
Electric fields
Joule heating
Lorentz forcing
Radiation
(UV, EUV)
E
Ne
PMSE:
Ion clusters
Aerosols
Ice particles
electron density
temperature
collisions
3-dim. wind field
Precipitation particles
Gravity wave generation
Heat conduction
Ionization
TURBULENCE:
Turbulent velocity
Intensity, morphology
Turbulent diffusion
Energy and momentum
deposition in mesosphere
by gravity waves
Gravity waves, tides:
generation, propagation
breaking, saturation
Momentum deposition of gravity
waves in the stratosphere
3-dim. wind field
Structure and dynamics of
polar stratospheric clouds
Turbulence and waves
Air flow
Tropopause folding
Polar tropopause
Polar
jet
Fine
structure
and laminae
in the tropo-
sphere and the
stratosphere
Gravity wave propagation
from the troposphere into
the stratosphere
Radar
Svalbard
Polar
vortex

Fig. 3

T2)

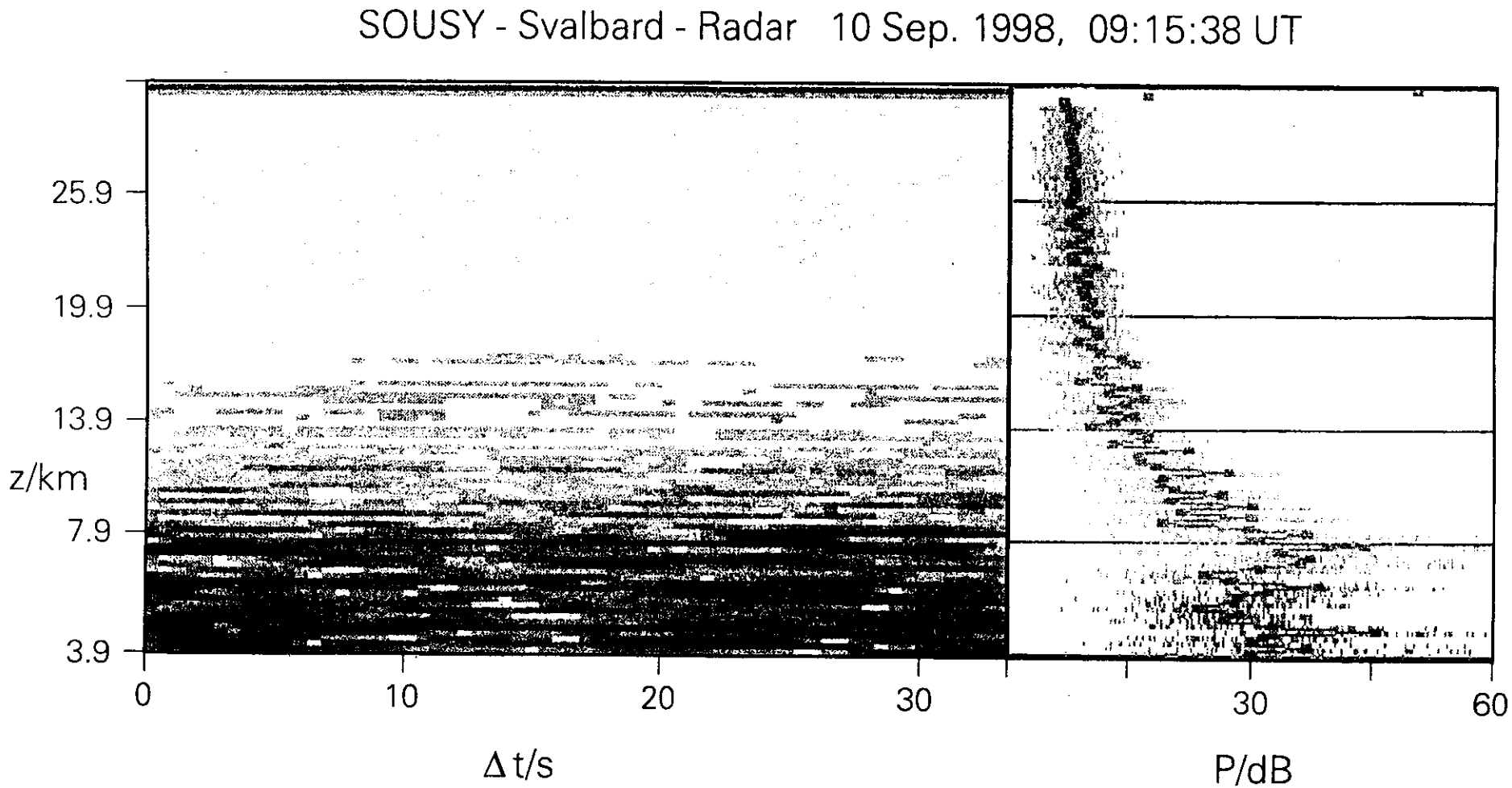
SOUSY - Svalbard - Radar 10 Sep. 1998, 09:15:38 UT
25.9
19.9
13.9
z/km
7.9
3.9
0
10
20
30
Δ t/s
30
60
P/dB

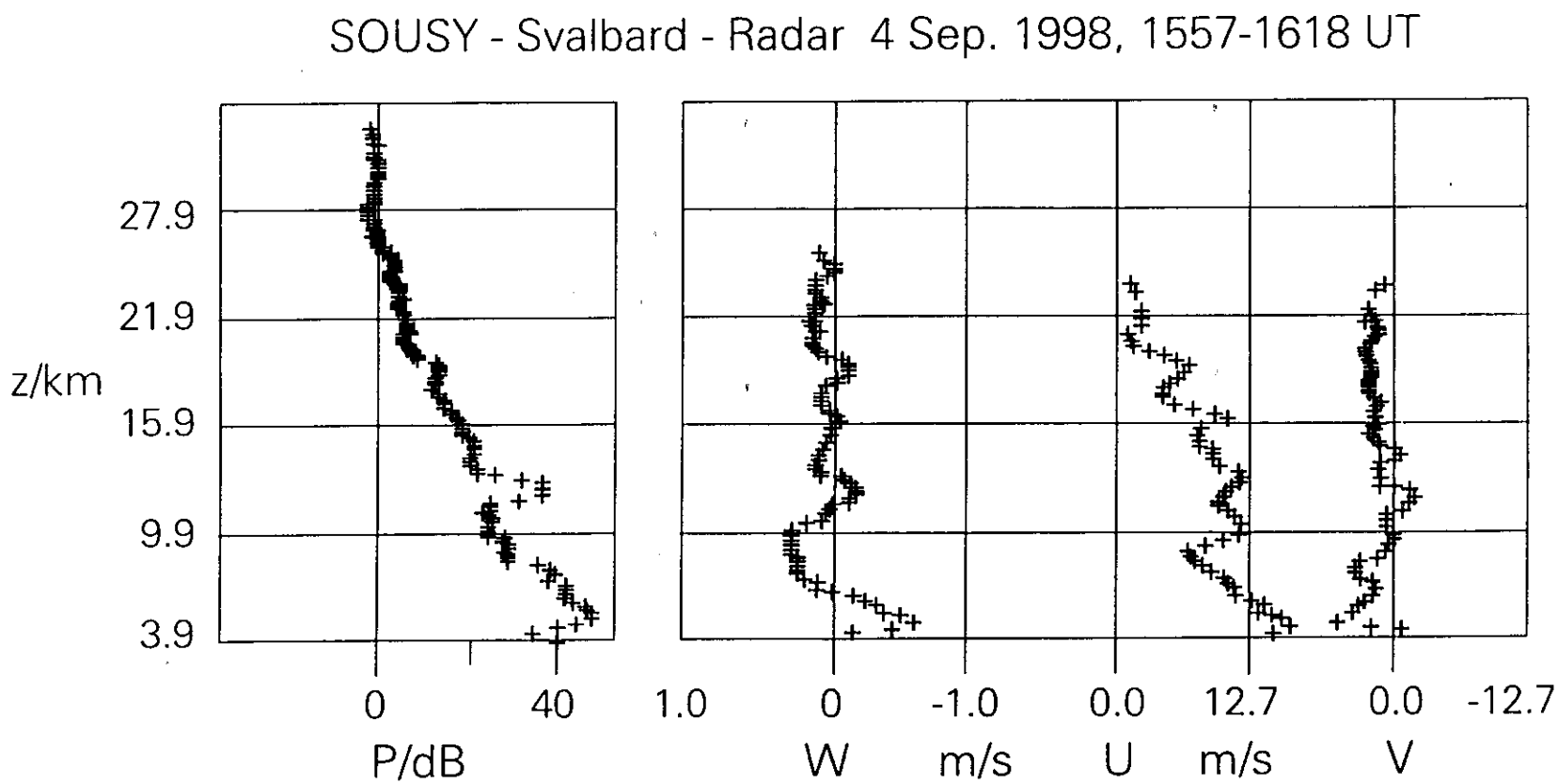
SOUSY - Svalbard - Radar 4 Sep. 1998, 1557-1618 UT
z/km
27.9
21.9
15.9
9.9
3.9
0
40
P/dB
1.0
0
-1.0
W
m/s
0.0
12.7
U
m/s
0.0
-12.7
V

SOUSY - Svalbard - Radar 13 - 14 Nov. 1999

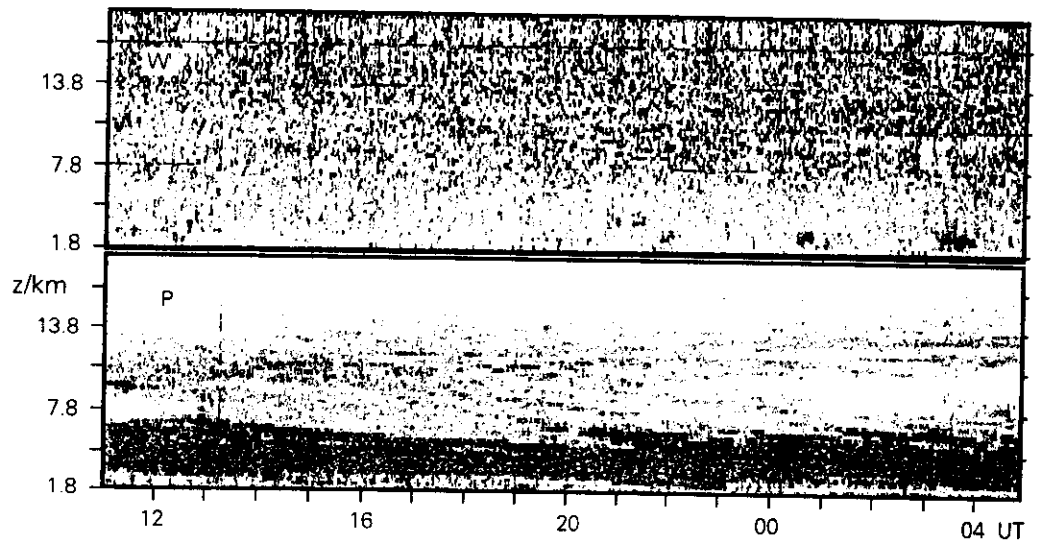

Fig.7

SOUSY - Svalbard - Radar 14 - 15 Nov. 1999

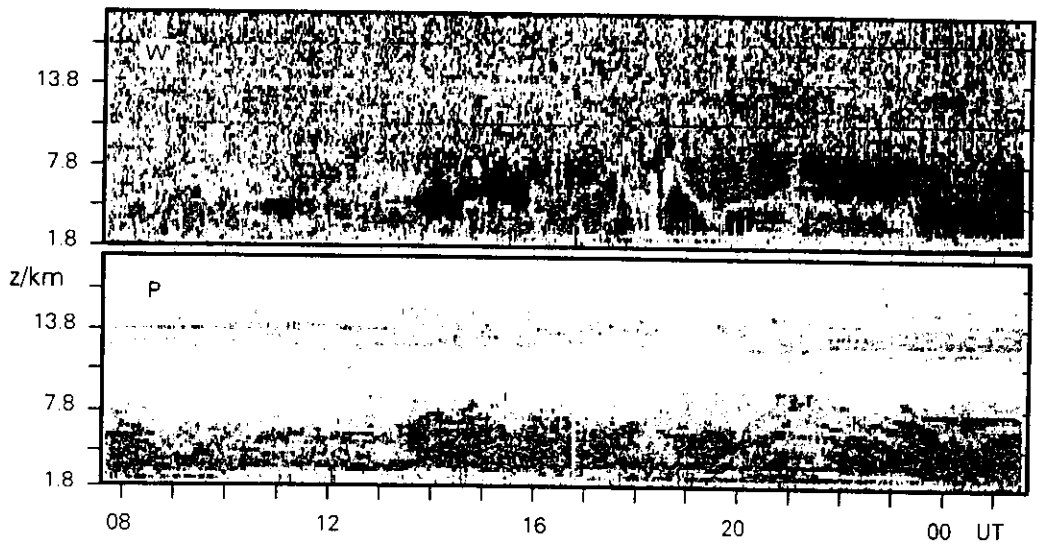

Fig.6

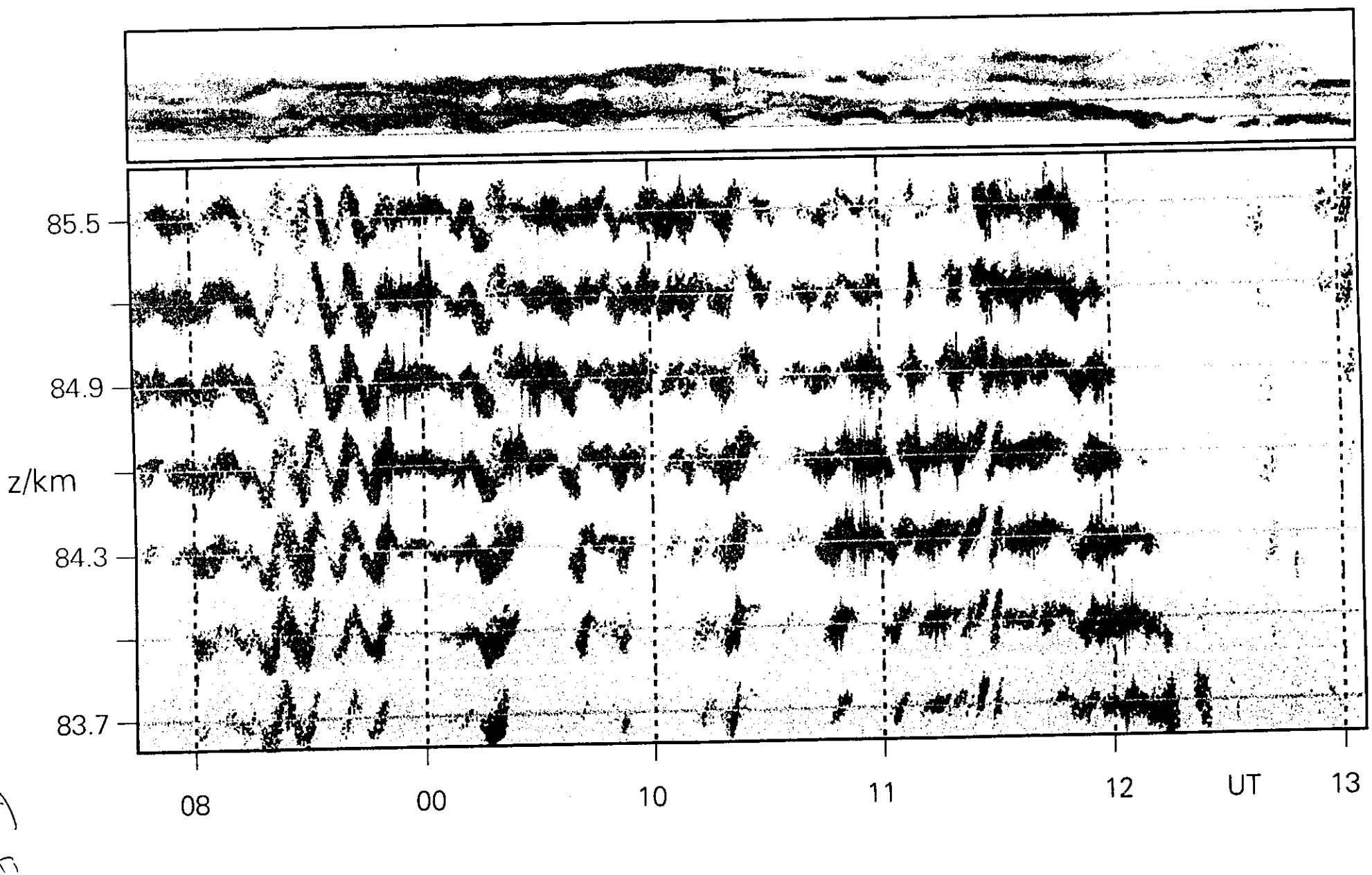
SOUSY - Svalbard - Radar PMSE 27 June 1999
85.5
84.9
z/km
84.3
83.7
08
00
10
11
12
UT
13

Fig. 8

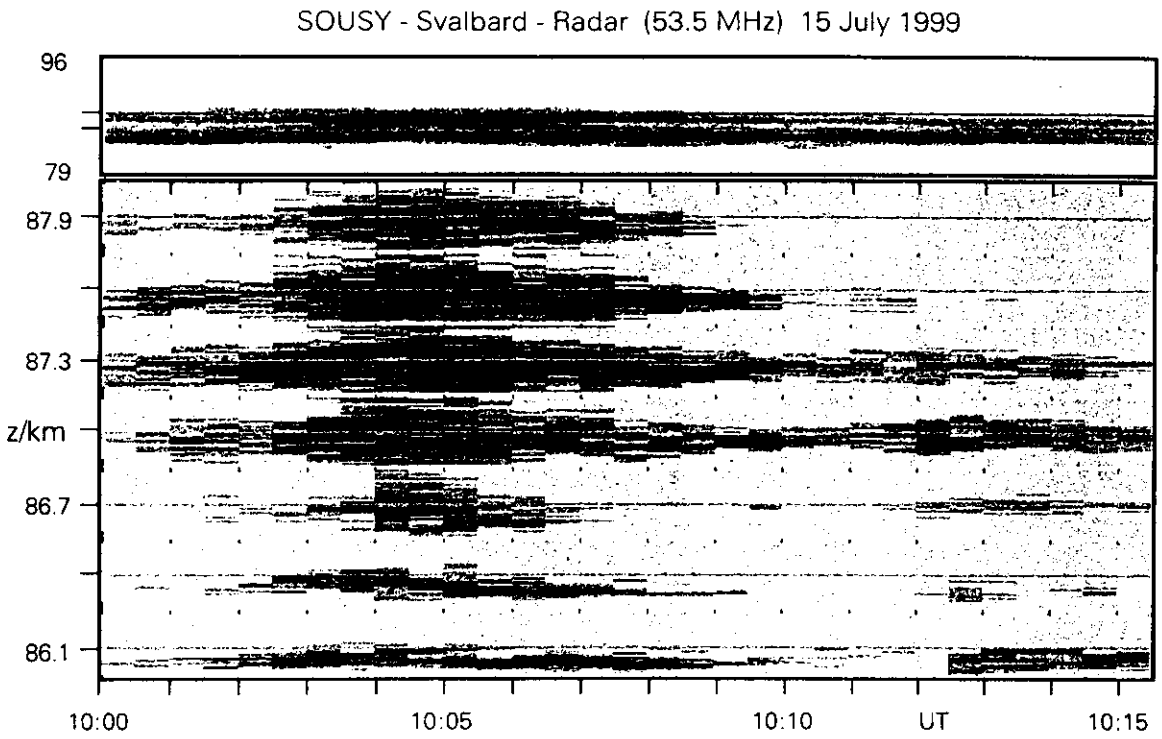
SOUSY - Svalbard - Radar (53.5 MHz) 15 July 1999
96
79
87.9
87.3
z/km
86.7
86.1
10:00
10:05
10:10
UT
10:15

Fig.

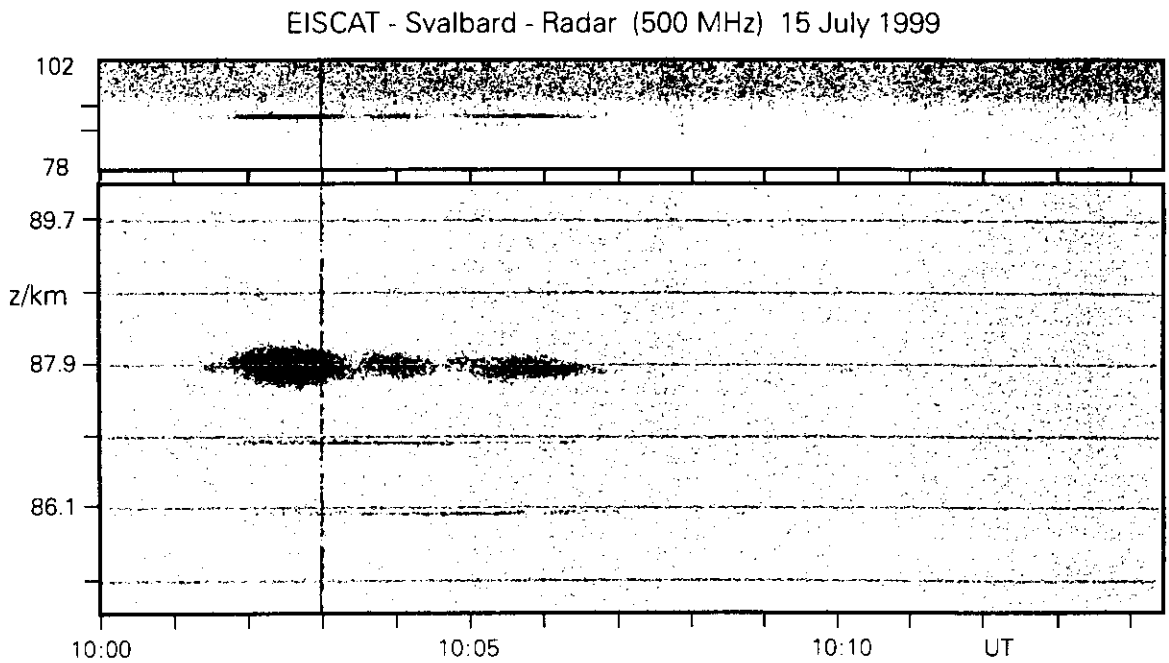
EISCAT - Svalbard - Radar (500 MHz) 15 July 1999
102
78
89.7
z/km
87.9
86.1
10:00
10:05
10:10
UT

Fig

T

EISCAT - Svalbard - Radar 24 Apr. 1998

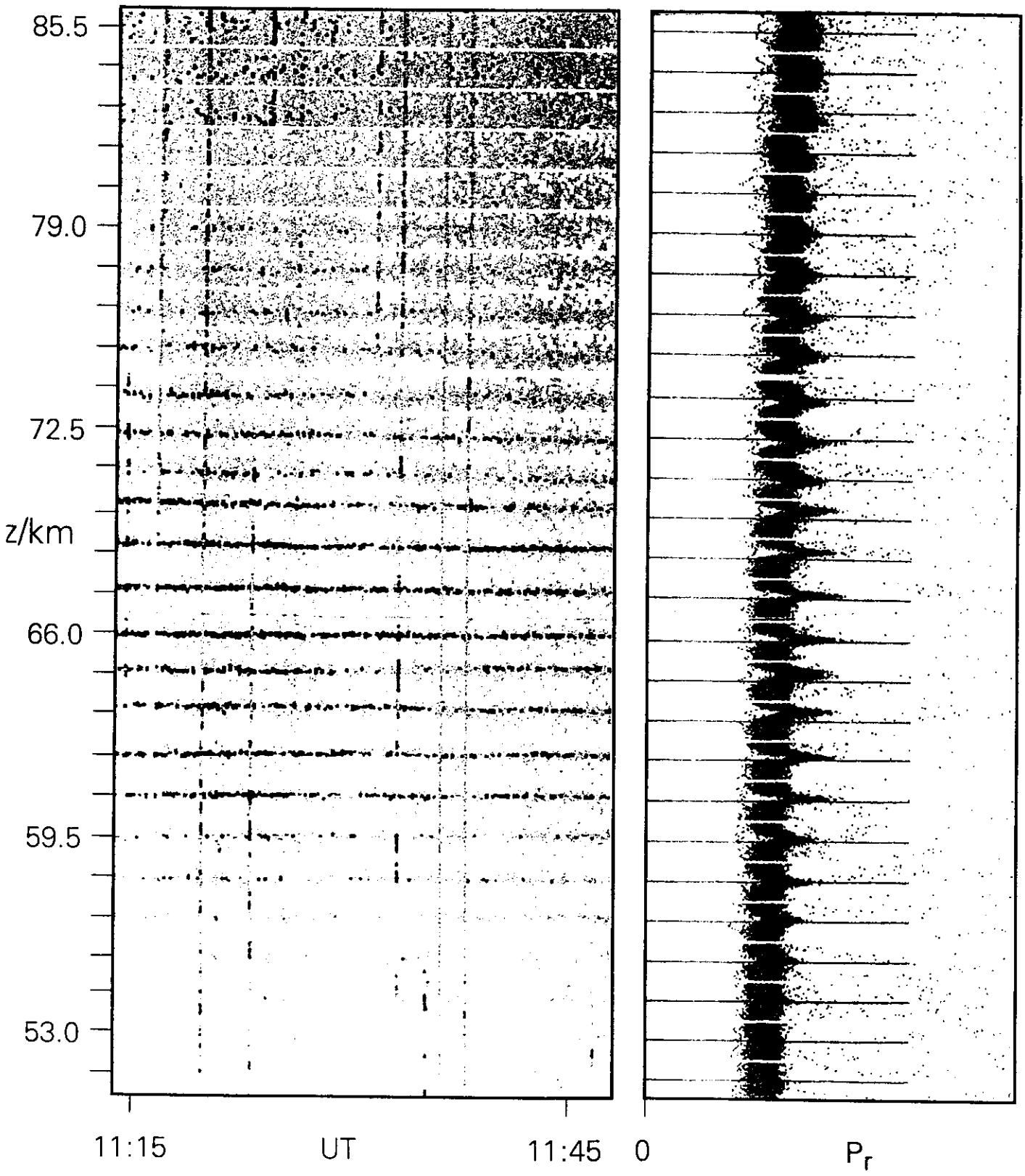

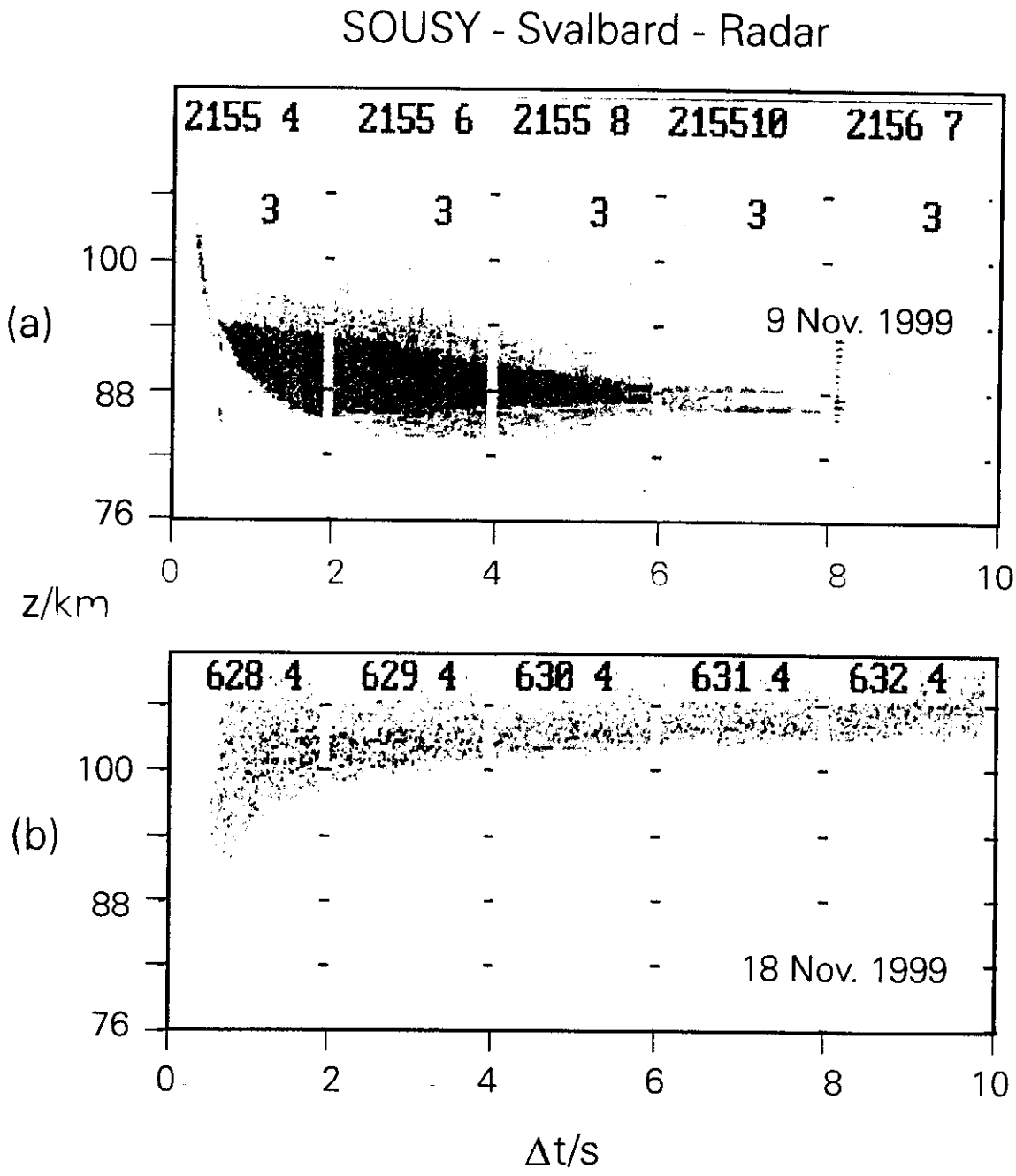
SOUSY - Svalbard - Radar
2155 4
2155 6
2155 8
215510
2156 7
3
3
3
3
3
100
88
76
(a)
9 Nov. 1999
0
2
4
6
8
10
z/km
628 4
629 4
630 4
631 4
632 4
100
88
76
(b)
18 Nov. 1999
0
2
4
6
8
10
Δt/s

Fig. 1